Effects of melt-blowing process conditions on morphological and mechanical properties of polypropylene webs

Youngchul Lee* and Larry C. Wadsworth
Textile Materials Research Laboratory, Center for Materials Processing, University of Tennessee, Knoxville, Tennessee 37996, USA
(Received 12 September 1990; revised 13 November 1990; accepted 13 November 1990)

Isotactic polypropylene (iPP) melt-blown webs have been studied in terms of the relationships among the processing conditions, structure and mechanical properties. The melt-blowing process conditions investigated in this study were die and air temperatures, die-to-collector distance (*DCD*) and attenuation air flow rate at the die. The macroscopic web structure was characterized in terms of interfibrous bonding and fibre diameter using scanning electron microscopy. The degree of fibre entanglements was found to increase with decreasing *DCD*, with increasing die temperature, or with increasing air flow rate. Using wide-angle X-ray diffraction and differential scanning calorimetry (d.s.c.), the microscopic molecular structure of iPP has been investigated. The fibres in a web consist of the α-form crystal, smectic phase and amorphous regions. The crystallinity of the iPP webs obtained from d.s.c. was found to be similar (39–44%) since the smectic phase transforms to crystals on heating in a d.s.c. A wide range of tensile properties and flexural rigidity values in the machine direction and cross direction were obtained at various processing conditions. The results have been analysed in terms of the degree of fibre entanglements, fibre orientation in the machine direction and the fraction of smectic phase.

(Keywords: polypropylene; melt-blowing process; web structure; fibre diameter; tensile property; flexural rigidity)

INTRODUCTION

Melt blowing has been one of the major processes to produce non-wovens since the last decade. The process was based on Wente's original work[1] and has been continuously studied[2–18]. A schematic diagram of the melt-blowing process is shown in *Figure 1*. In this process, a thermoplastic polymer is extruded through a die containing a row of several hundred closely spaced small spinnerets. The extruded polymer melt is attenuated by convergent streams of hot air at the die tip (*Figure 1*) and forms a three-dimensional entangled-fibre web, which is collected on a porous cylinder or conveyor belt. Thus, melt-blown non-woven fabrics are produced directly from granules or pellets of thermoplastics in one step.

At relatively low polymer throughput rates and at high air flow rates, webs with smaller-diameter fibres are usually produced. The primary object of this study was to determine if similar mechanical properties of the web could be produced at higher die and air temperatures and with lower air flow rates, to conserve air compressor energy. A previous study by Milligan *et al.*[14] revealed that the major energy cost in melt blowing was in providing compressed air for the die.

Owing to the microdenier fibrous web sructure, melt-blown fabrics are ideally suited for filtration media, thermal insulators, battery separators and oil sorbents. The average fibre diameter of a typical melt-blown web is only a few micrometres, compared with typical textile fibres ranging from 15 to 50 μm. Nevertheless, webs with fibre diameters greater than 10 μm can also be produced to meet specific applications.

Although the contributions of melt-blown fabrics to various applications have been growing rapidly[19], their weak mechanical properties often limit the application. To improve the mechanical properties of melt-blown fabrics, the relationships between the processing conditions and physical properties have been investigated. This study will also be useful in optimizing the melt-blowing process for a specific end-use.

EXPERIMENTAL

Materials

A commercial isotactic polypropylene (iPP) resin in pellet form (700 nominal melt flow rate) produced by Exxon Chemical Company for melt blowing was used. The resin has an intrinsic viscosity of 0.73 dl g^{-1}, M_w of 93000 and M_n of 27000 according to gel permeation chromatography analyses performed by the Exxon Chemical Company, Baytown Polymer Products Center, Baytown, Texas.

Melt-blowing process

The melt blowing was performed on the 20 inch (0.51 m) melt-blowing line at the University of Tennessee,

* To whom correspondence should be addressed at current address: Korea Academy of Industrial Technology, 790-2, Yoksam-dong Kangnam-Ku, Seoul 135-080, Korea

0032-3861/92/061200-10

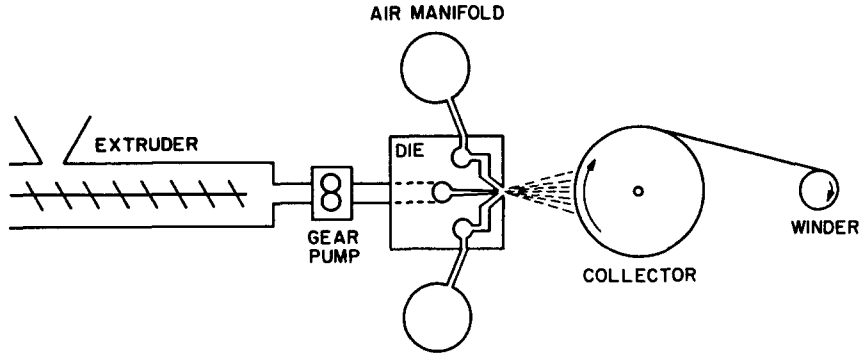

Figure 1 Schematic melt-blowing pilot line at the University of Tennessee

Table 1 Melt-blowing processing conditions at a polymer throughput rate of 0.4 g min^{-1} per hole

Die temp. (°C)	Extruder temp. (°C)	Air temp. at die (°C)	Air flow rate (ft^3 min^{-1})	Air flow rate (m^3 min^{-1})	Die-to-collector distance, *DCD* (m)	Sample code[a]
207	175–193	210	160	4.5	0.16, 0.30, 0.61	L-50
			260	7.4	0.16, 0.30, 0.61	L-65
			370	10.4	0.16, 0.30, 0.61	L-75
230	175–215	224	160	4.5	0.16, 0.30, 0.61	M-50
			260	7.4	0.16, 0.30, 0.61	M-65
			370	10.4	0.16, 0.30, 0.61	M-75
246	182–243	243	160	4.5	0.16, 0.30, 0.61	H-50
			260	7.4	0.16, 0.30, 0.61	H-65
			370	10.4	0.16, 0.30, 0.61	H-75

[a]Letters L, M and H correspond to low, medium and high die temperatures, respectively; and 50, 65 and 75 correspond to per cent air valve opening required to achieve the air flow rates shown

Knoxville (UTK), Textile Processing Laboratory. The line consists of a 2.0 inch (30/1 *L/D*) extruder, a two-position screen changer, a gear metering pump, a 20-inch-wide die with 401 spinneret orifices of approxi mately 0.4 mm diameter, an electric furnace for heating the air, and a rotary-screw air compressor with maximum capacity of 650 standard ft^3 min^{-1} (18.4 m^3 min^{-1}). Actual air flow rates of 160, 260 and 370 standard ft^3 min^{-1} (4.5, 7.4 and 10.5 m^3 min^{-1}) corresponding to 50, 60 and 75% air valve opening setting on the gate valve from the compressor, respectively, were used.

The three different sets of processing temperatures studied are given in *Table 1*. The temperatures of the die, air and several heating zones between the feeding zone and the die were changed in the same manner. Therefore the die temperature can be considered as the processing temperature. The letters L, M and H in the sample codes in *Table 1* correspond to low (207°C), medium (230°C) and high (246°C) die temperatures, respectively. Die-to-collector distances (*DCD*) of 6.25 inch (0.16 m), 12 inch (0.30 m) and 24 inch (0.61 m) were used to prepare a web with an average basis weight of 1.0 oz yd^{-2} (33.9 g m^{-2}) at a constant polymer throughput rate of 0.4 g min^{-1} per hole. The three chosen conditions for the three processing conditions, i.e. die temperature, air flow rate and *DCD*, are considered to cover a large portion of the entire processing range for the polypropylene used.

Thickness and basis weight

Thickness of melt-blown webs was measured by using the Ames Thickness Gauge, model 85-0071 (Testing Machines Inc), in accordance with ASTM test method D1777-64[20]. The samples had thickness values ranging from 0.26 to 0.56 mm as shown in *Table 2*. Basis weight was measured according to ASTM test method D3776-79[20]. The average basis weight of the samples produced was 1.0 oz yd^{-2} (33.9 g m^{-2}).

Scanning electron microscopy

Polypropylene web structure was observed using an ETEC Auto-scan scanning electron microscope at 20 keV after the sample had been coated with a gold layer. For fibre diameter measurements, photomicrographs were taken of five different positions for each web. Latex particles of 2.68 ± 0.014 μm diameter were used for calibration of magnification.

Mechanical properties

Strips of 25.4 mm × 178 mm with the long dimension along the machine direction (MD) and cross direction (CD) were cut from each web and weighed. At least 10 samples in each direction (MD or CD) were used for tensile property and flexural rigidity measurements. Tenacity and elongation to break of the melt-blown webs were measured using an Instron tensile tester in accordance with ASTM standard test methods D1117-80 and D1682-64[20], and INDA standard test IST 110.0-70(R82)[21]. A gauge length of 127 mm, a head speed of 127 mm min^{-1} and, therefore, a strain rate of 1.0 min^{-1} was used. Flexural rigidity was measured by using a Cantilever Bending Tester (Testing Machines Inc.) according to ASTM D1388-64[20].

Table 2 Various physical properties of melt-blown polypropylene webs

Sample code	DCD (m)	DCD (inch)	Thickness (mm)	Fibre diameter Average[a] (μm)	Fibre diameter S.d. (μm)	Tensile property MD Tenacity (g denier^{-1})	MD Elongation to break (%)	CD Tenacity (g denier^{-1})	CD Elongation to break (%)	Flexural rigidity MD	Flexural rigidity CD	Flexural rigidity Average[b] (mg cm)
L-50	0.16	6.25	0.55	19.1	2.9	0.100	21.1	0.074	23.3	384	242	305
	0.30	12	0.55	18.5	3.9	0.086	25.5	0.073	29.3	363	249	301
	0.61	24	0.56	20.0	4.6	0.055	31.6	0.053	36.0	319	193	248
L-65	0.16	6.25	0.50	12.9	4.0	0.127	17.8	0.092	18.2	475	366	417
	0.30	12	0.48	13.4	4.1	0.105	28.0	0.089	32.3	403	233	306
	0.61	24	0.51	13.8	4.5	0.074	41.0	0.068	46.7	462	202	305
L-75	0.16	6.25	0.48	9.9	3.1	0.126	13.9	0.093	16.6	814	471	619
	0.30	12	0.48	9.6	3.4	0.107	35.7	0.092	43.7	410	310	357
	0.61	24	0.52	10.9	4.5	0.074	57.9	0.074	60.0	303	305	304
M-50	0.16	6.25	0.53	17.5	3.9	0.084	9.8	0.066	11.4	388	327	356
	0.30	12	0.53	16.3	4.0	0.085	16.5	0.075	23.0	370	280	322
	0.61	24	0.56	17.7	4.5	0.059	24.2	0.055	29.7	362	190	262
M-65	0.16	6.25	0.41	8.9	4.0	0.130	7.1	0.078	9.5	706	333	485
	0.30	12	0.41	8.7	4.6	0.114	29.4	0.094	39.7	394	259	319
	0.61	24	0.49	8.8	4.8	0.064	44.8	0.070	49.7	224	206	215
M-75	0.16	6.25	0.39	7.7	3.9	0.148	5.3	0.085	8.2	917	420	621
	0.30	12	0.39	8.0	3.4	0.121	23.1	0.096	41.3	480	332	399
	0.61	24	0.46	7.9	3.5	0.065	50.3	0.070	57.5	222	247	234
H-50	0.16	6.25	0.48	11.0	4.6	0.079	5.4	0.049	5.2	627	343	464
	0.30	12	0.43	12.1	4.1	0.095	10.4	0.077	14.0	473	245	340
	0.61	24	0.57	11.3	4.0	0.058	16.5	0.058	19.3	396	247	313
H-65	0.16	6.25	0.28	5.5	2.7	0.141	3.5	0.060	3.2	685	390	517
	0.30	12	0.34	6.6	2.9	0.141	19.8	0.086	39.3	610	383	483
	0.61	24	0.46	6.3	3.2	0.064	34.8	0.064	48.0	279	266	272
H-75	0.16	6.25	0.26	4.5	2.9	0.197	4.2	0.064	3.5	1192	326	623
	0.30	12	0.33	5.8	4.0	0.135	25.0	0.100	70.2	512	289	385
	0.61	24	0.39	5.9	3.8	0.067	47.0	0.074	67.6	86	83	84

[a]Arithmetic average
[b]Geometric average

Differential scanning calorimetry

Melting behaviours of melt-blown iPP webs were characterized with a Perkin–Elmer differential scanning calorimeter (DSC-7) calibrated with the melting transitions of indium and tin. All measurements were performed at a heating rate of 20°C min^{-1} in nitrogen.

Wide-angle X-ray diffraction

A Rigaku-Denki X-ray diffractometer equipped with a pulse-height counter was used to characterize the molecular structure in polypropylene fibres. The experiment was performed in reflection mode with Ni-filtered Cu Kα radiation at 35 kV and 30 mA.

RESULTS AND DISCUSSION

Web structure

The macroscopic web structures of isotactic polypropylene (iPP) melt-blown fabric have been studied. A typical melt-blown polypropylene fabric has an entangled-fibre web structure as shown in *Figure 2*. The arrow in *Figure 2* indicates the machine direction (MD). Fibres tend to orient to MD, resulting in anisotropic physical properties. The fibres observed by a scanning electron microscope (SEM) were essentially round and rod-like in shape. The diameters of individual fibres in the web appear to change along the length of the fibres. Filaments coming out from the melt-blowing die become entangled with several others between the die and collector. Fibre-entanglement is believed to be enhanced by the attenuation air streams coming through the gaps above and below the row of spinnerets (*Figure 1*).

In *Figure 3*, the effects of *DCD* on web structure is shown. In the web produced at 0.16 m, individual fibres are not well defined owing to a high degree of interfibre bondings. Although the mechanism of web formation is not understood completely, at least three kinds of interfibre bonding or fibre entanglements are observed in melt-blown webs[2]. These are thermal sticking, branching and interlacing, and their total population or the degree of fibre entanglement are used to describe a melt-blown web[2]. If the entangled fibres are not quenched enough they may be fused together and lose their identity, which often makes it hard to tell the origin of the fibre junctions. As *DCD* was increased, the degree of fibre entanglement decreased. The web produced at a short *DCD* is expected to be strong and stiff owing to the high degree of fibre entanglement.

Figure 4 shows SEM micrographs of the webs produced at a *DCD* of 0.30 m and an air flow rate of 10.5 m^3 min^{-1}. As the die temperature was increased, the web exhibited more interfibre bonds with irregular fibre diameters. The average fibre diameter decreased with increasing processing temperature, which was also found for all the other samples produced at different *DCD*

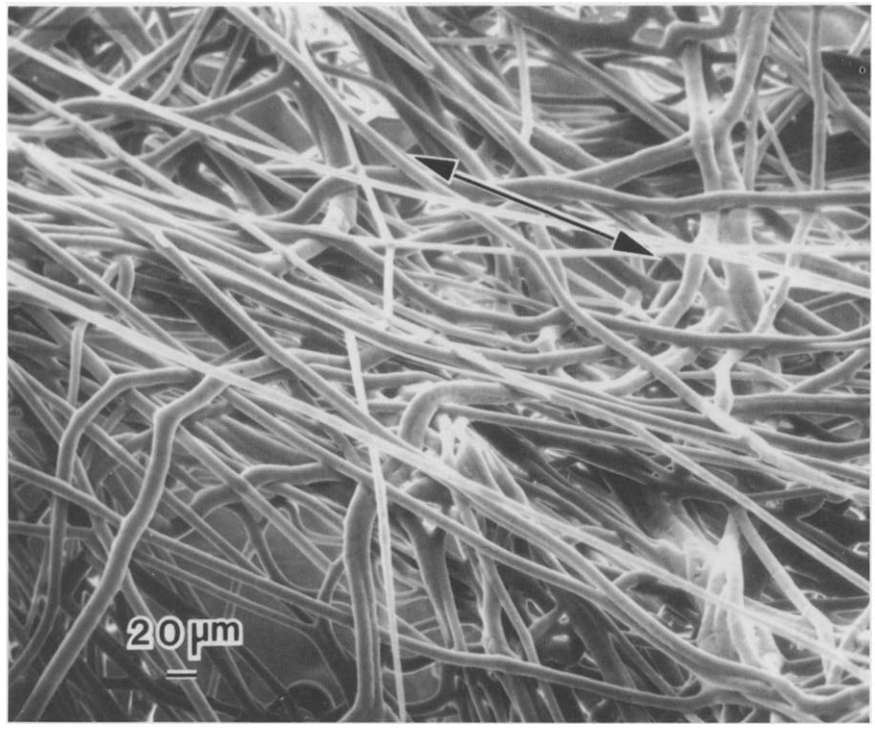

Figure 2 Scanning electron micrograph of a polypropylene web produced at a die temperature of 207°C, an air flow rate of 7.4 $m^3 min^{-1}$ and a *DCD* of 0.16 m. Arrow indicates the machine direction

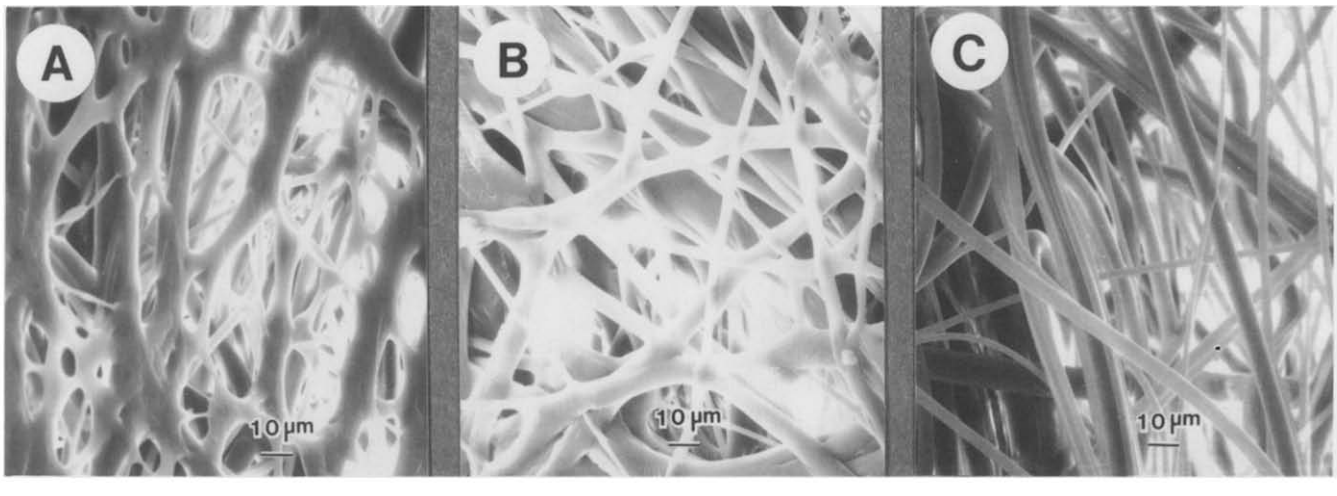

Figure 3 Scanning electron micrographs of polypropylene webs melt blown at 246°C and 10.5 $m^3 min^{-1}$ as a function of *DCD*: (A) 0.16 m; (B) 0.30 m; (C) 0.61 m

and air flow rates. The average fibre diameter was obtained from a previous study[2] and is listed with the standard deviation in *Table 2*. The large values of standard deviations of fibre diameter for melt-blown webs are typical regardless of the process conditions studied here and indicate the broadness of the fibre diameter distribution.

Figure 5 shows SEM micrographs of webs at different attenuation air flow rates. The webs produced at a low air flow rate (A) show more or less periodically creased skins probably owing to less drawing at the low air flow rate. The creased skin is observed on some fibres in B; however, not in C. Fibre diameter decreased remarkably with increasing air flow rates. The stress, or the dragging force, generated by the attenuation air reduces the fibre diameter. It appears that air flow rates greater than 7.4 $m^3 min^{-1}$ are required to reduce fibre diameter effectively at a die temperature of 230°C. As listed in *Table 2*, the fibre diameter always decreased with increasing attenuation air flow rate at the die.

Observations from *Figures 3–5* are as follows. The fibre orientation along MD was observed to increase with increasing air flow rate or with decreasing *DCD*. As *DCD* was increased, the degree of fibre entanglement decreased. As either the die temperature or air flow rate was increased, the degree of fibre entanglement increased and the average fibre diameter decreased. A melt-blown web with a high degree of fibre entanglement or a small average fibre diameter is expected to show a small pore size, which indeed was previously found using a

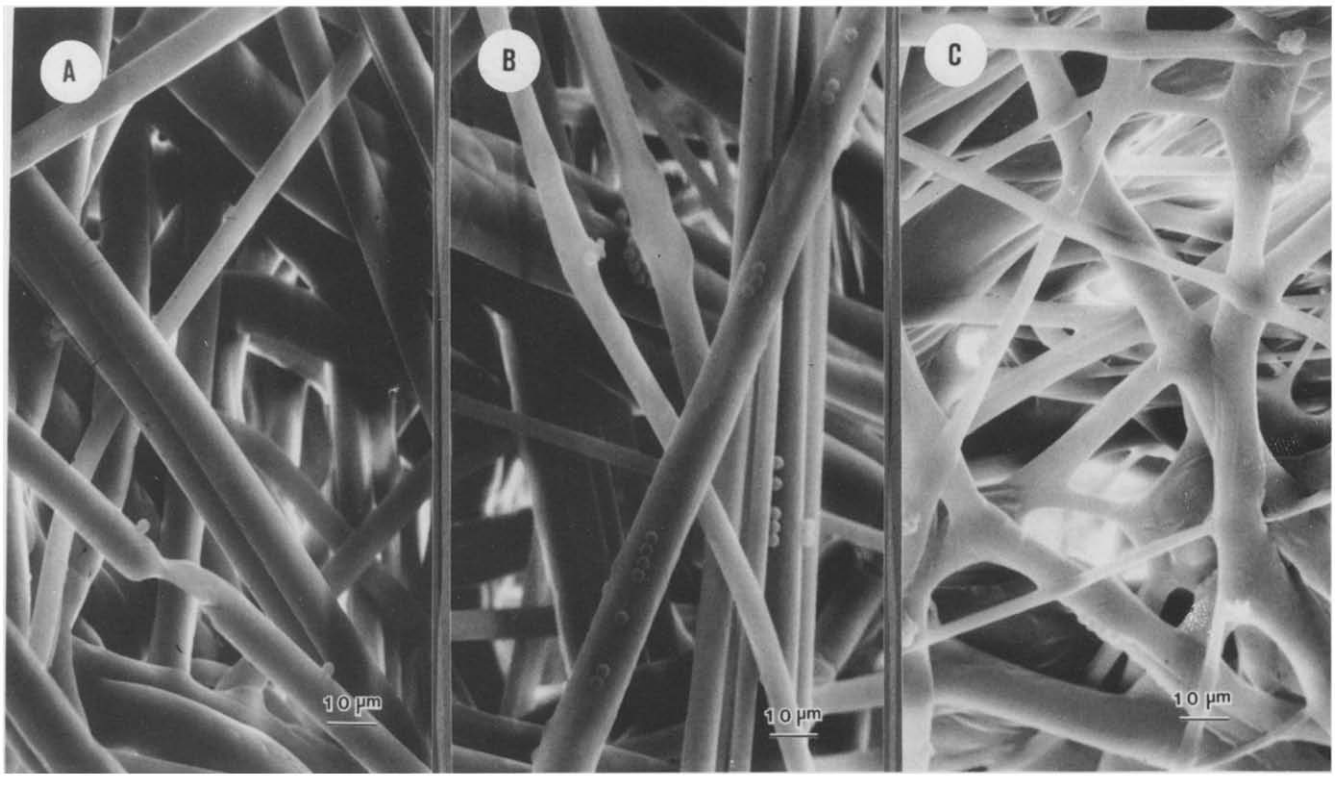

Figure 4 Scanning electron micrographs of polypropylene webs melt blown at 10.5 $m^3 min^{-1}$ and 0.30 m as a function of die temperature: (A) 207°C; (B) 230°C; (C) 246°C. The spheres in the figures are polystyrene latex particles for magnification calibration

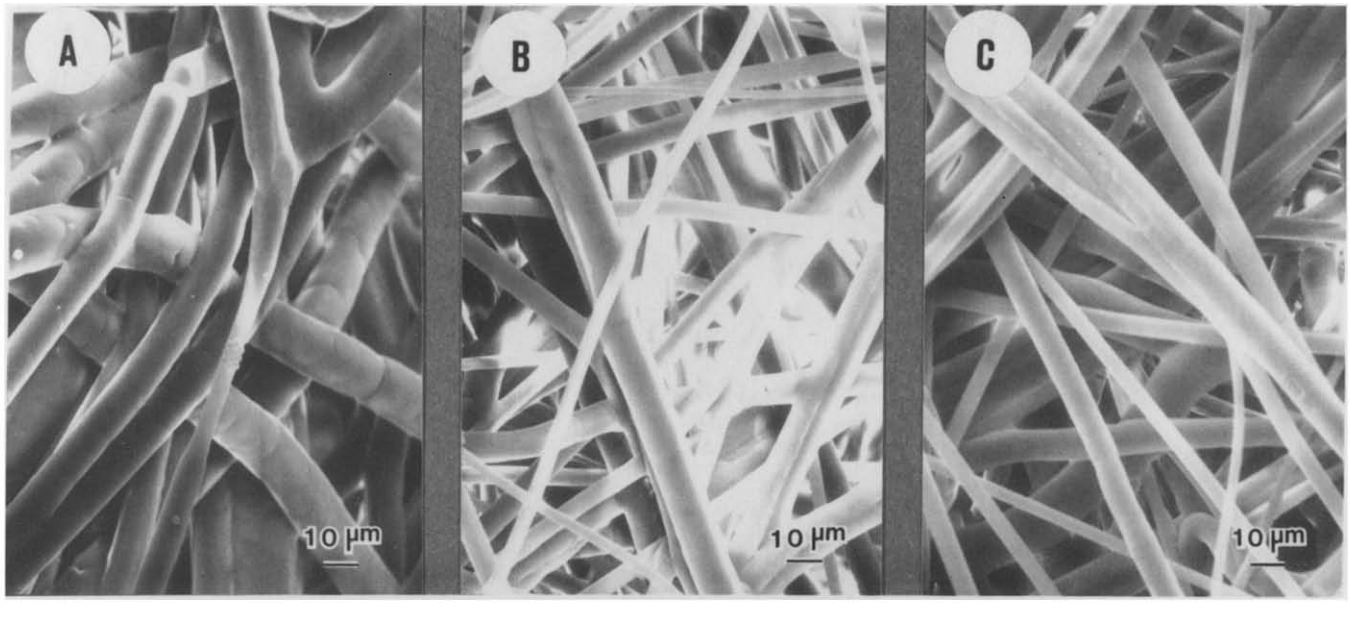

Figure 5 Scanning electron micrographs of polypropylene webs melt blown at 230°C and 0.30 m as a function of air flow rate: (A) 4.5 $m^3 min^{-1}$; (B) 7.4 $m^3 min^{-1}$; (C) 10.5 $m^3 min^{-1}$. The spheres in the figures are polystyrene latex particles for magnification calibration

Porometer[2]. The web with small pores also showed a high latex filtration efficiency and a low air permeability[2].

Mechanical properties of melt-blown webs

Figure 6 shows stress–strain curves of webs produced at 230°C in MD. The webs produced at a die-to-collector distance (*DCD*) of 0.16 m showed high tenacity (tensile strength), high modulus and brittle fracture owing to the high degree of fibre entanglement as shown in *Figure 3*. As the *DCD* was increased, the brittle fracture changed to ductile fracture especially for the webs produced at higher air rates. As the attenuation air flow rate was increased, the web showed a greater tenacity and a greater modulus. Comparing the tensile properties of the webs produced at the three air flow rates in *Figure 6*, the melt blowing at a higher air flow rate produces a wider range of tensile properties by changing *DCD*. *Figure 6* also indicates the versatility of the melt-blowing process since

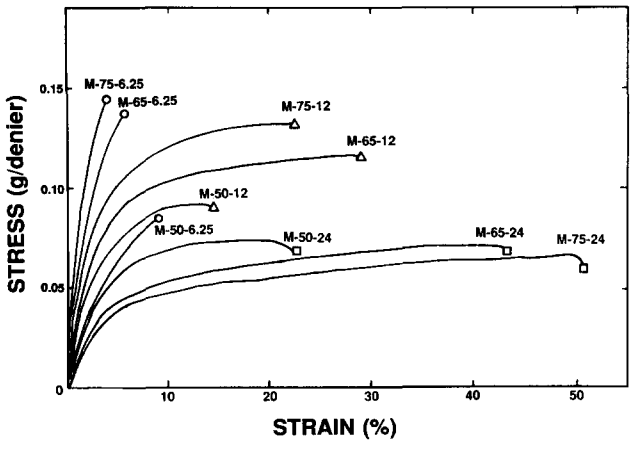

Figure 6 Stress–strain curves of polypropylene webs melt blown at 230°C

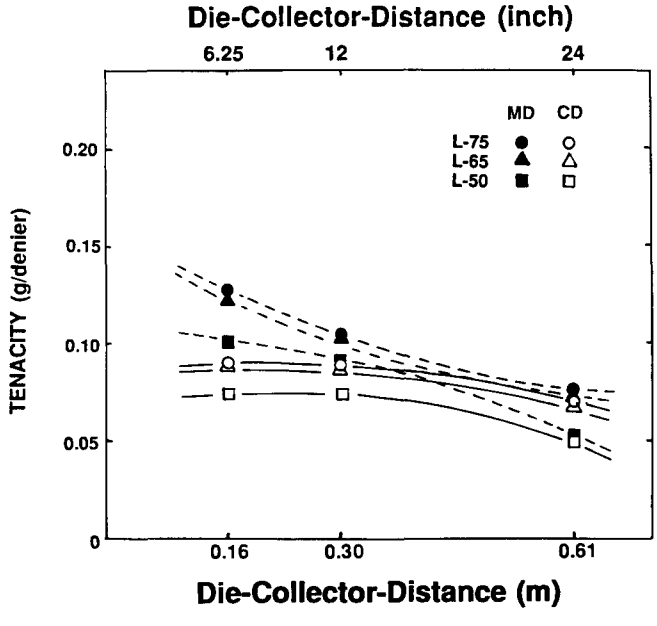

Figure 7 Tenacity of polypropylene webs melt blown at 207°C

it is easy to change the air flow rate and *DCD* without stopping the production line.

Figures 7–9 show tenacities in MD and CD for webs produced at 207, 230 and 246°C, respectively. MD tenacity was greater than CD tenacity except for the webs produced at a long *DCD*. This is explained since the fibre orientation along MD is significant, unless the web is produced at a long *DCD*, like 0.61 m. At a low die temperature of 207°C (*Figure 7*) the tenacities in MD and CD decrease slightly with increasing *DCD* or with decreasing air flow rate. As air flow rate was increased, the tenacities in MD and CD slightly increased. In *Figures 8* and *9*, the MD tenacity of webs produced at 230 or 246°C generally decreased with increasing *DCD* and with decreasing air flow rate. The tenacity in CD at high processing temperatures shows a maximum around a *DCD* of 0.30 m. The tenacity difference in MD and CD, which is considered to be mostly due to orientation of fibres along MD, appears to be great at a short *DCD* and at a high air flow rate.

Comparing *Figures 7*, *8* and *9*, it is noted that the effects of the attenuation air on MD tenacity become greater as the die temperature is increased. The effects of the attenuation air flow on the CD tenacity, however, are similar regardless of the die temperatures used. The effects of the die temperature on MD and CD tenacities are different depending on *DCD* and air flow rate. The MD tenacity of the webs produced at a short *DCD* and at a high air flow rate showed the greatest dependence on the die temperature; the MD tenacity increased but CD tenacity decreased, with increasing die temperature. This indicates that the three major melt-blowing processing conditions, i.e. die temperature, attenuation air flow rate at the die and *DCD*, are closely interrelated.

In *Figure 10*, the elongation to break for webs produced at 230°C are plotted *versus DCD*. The elongation to break in CD is greater than that in MD, and the elongation to break in MD and CD increased with increasing *DCD* for all the webs studied. The effects of the attenuation air flow on the elongation appeared to be dependent on *DCD*; with increasing air flow rate, the elongation decreased at a short *DCD* but it increased

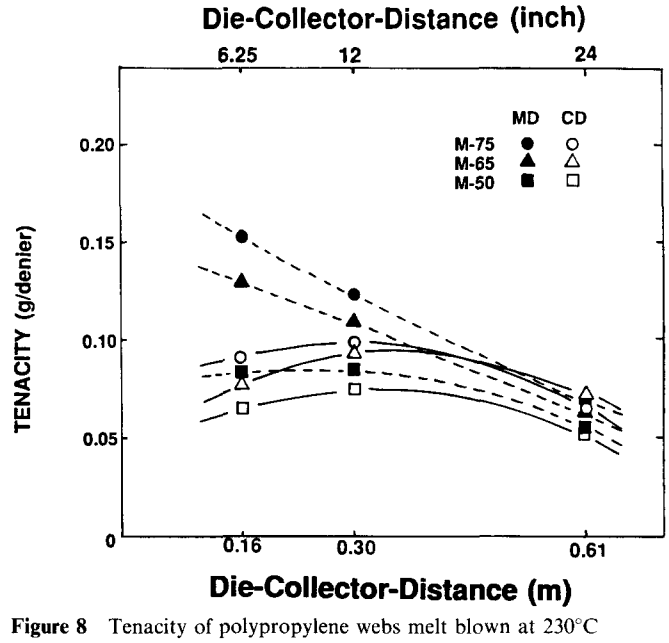

Figure 8 Tenacity of polypropylene webs melt blown at 230°C

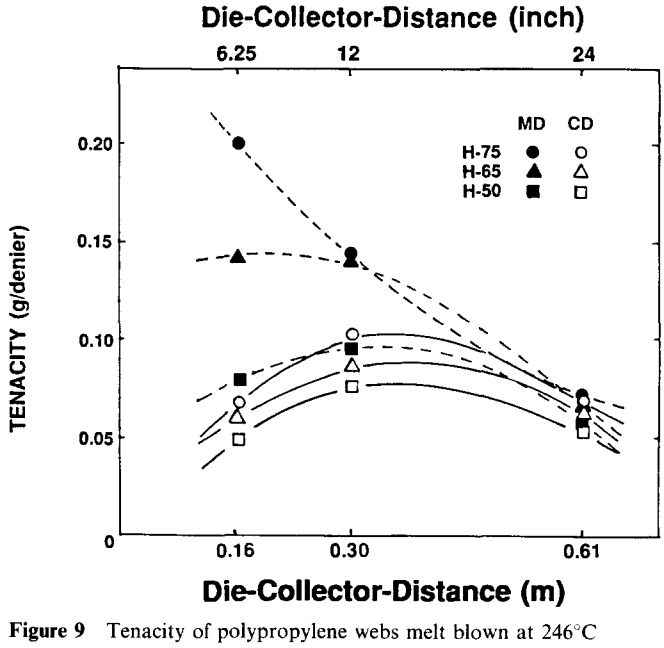

Figure 9 Tenacity of polypropylene webs melt blown at 246°C

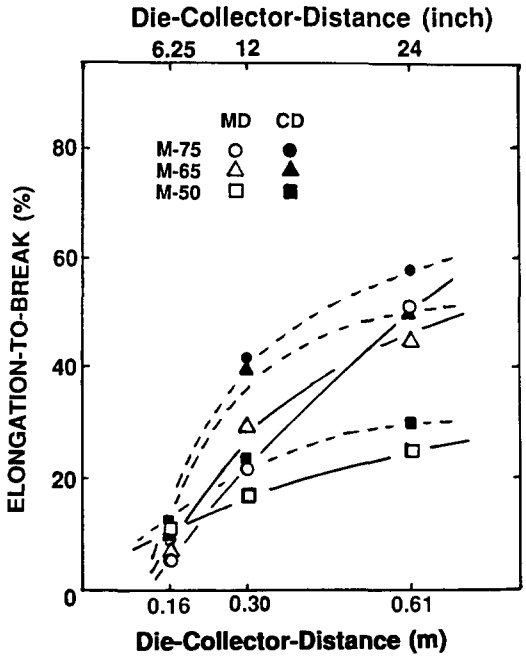

Figure 10 Elongation to break of polypropylene webs melt blown at 230°C

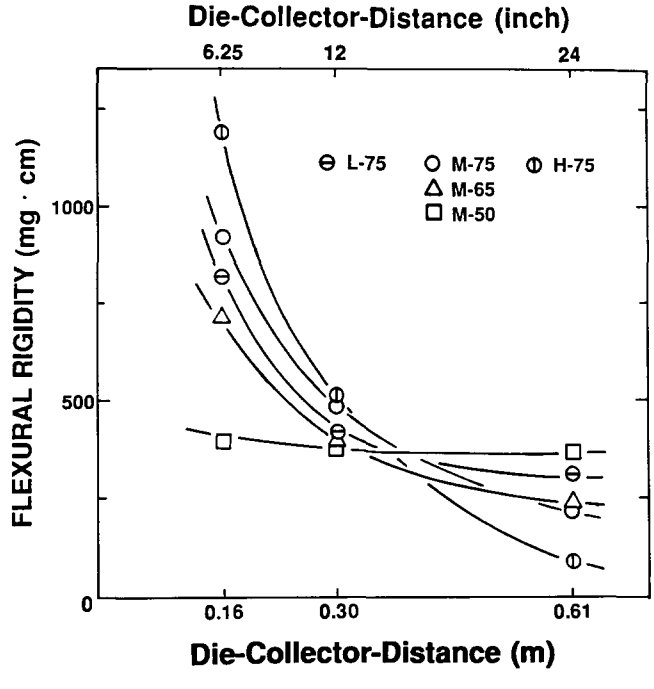

Figure 11 Bending rigidity in the machine direction (MD) of melt-blown polypropylene webs

at a long *DCD*. These behaviours were also observed for the samples produced at 207 and 246°C as listed in *Table 2*. It is also noted that the elongation to break decreased with increasing die temperature, which is considered to be due to increased interfibre bonding. The tensile properties of a single filament from a web were previously compared with those of the web[13,18]. The elongation to break, tenacity and modulus of the single fibre were greater than those of the web, suggesting that tensile failure probably occurs through interfibre bonding rather than through individual fibres.

Flexural (bending) rigidities in MD and CD were measured using a Cantilever Bending Tester and plotted *versus DCD* in *Figures 11* and *12*, respectively. Flexural rigidity is a measure of stiffness of a fabric. A lower value of flexural rigidity indicates high drapability and flexibility, which is good for clothing and internal design applications. Generally, flexural rigidity in MD decreased with *DCD*, which has been previously observed for PP of different molecular weights at different processing conditions[13]. Flexural rigidity is considered to be dependent on the degree of fibre entanglement, fibre orientation and fibre diameter. A fibre entanglement junction acts as a reinforcing point of the flexible fibres. The degree of fibre entanglement clearly decreased as *DCD* increased (*Figure 3*), which might be the major reason for the decrease in the rigidity with increased *DCD* (*Figures 11 and 12*). A web produced at a low air flow rate, however, showed little change in the flexural rigidity with *DCD*. As the die temperature was increased, MD rigidity (*Figure 11*) of the web produced at a short *DCD* increased. However, MD rigidity of the webs produced at a long *DCD* decreased. Little difference in CD rigidity was observed for webs produced at various air flow rates, or at various die temperatures. The geometric average of MD and CD flexural rigidities, which is recommended by ASTM D1388-64[20] is also listed in *Table 2*. The average flexural rigidity, in general, decreases with increasing *DCD* or decreasing air flow rate.

Microstructure of melt-blown fibres

Polymer melt comes out from the melt-blowing die and crystallizes while the continuous filaments form a web structure. The melting behaviour of the crystals of the melt-blown PP web was characterized using differential scanning calorimetery (d.s.c.). *Figure 13* shows d.s.c. traces of various webs produced at an air flow rate of 10.5 m^3 min^{-1}. The top three d.s.c. curves show the effects of the die temperature. As the die temperature was increased, the peak temperature of the melting endotherm slightly shifted to a higher temperature and the 'shoulders' on the endotherm became more distinctive. These 'shoulders' are considered to be

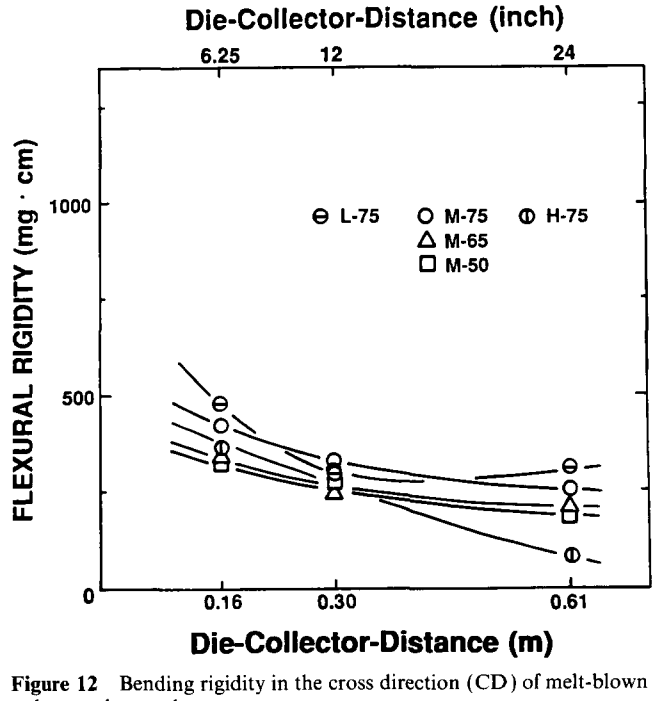

Figure 12 Bending rigidity in the cross direction (CD) of melt-blown polypropylene webs

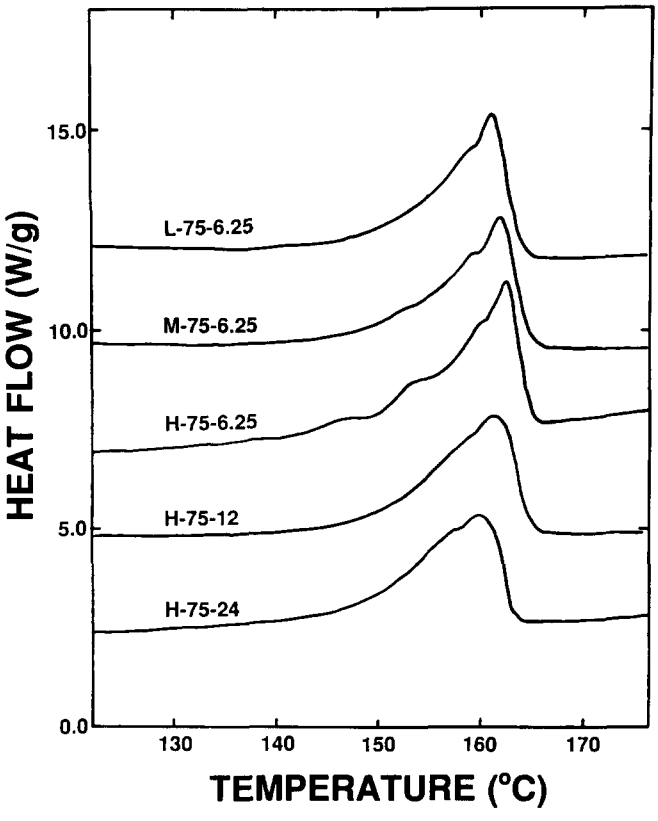

Figure 13 Differential scanning calorimetry traces of melt-blown polypropylene webs. Heating rate was 20°C min^{-1}

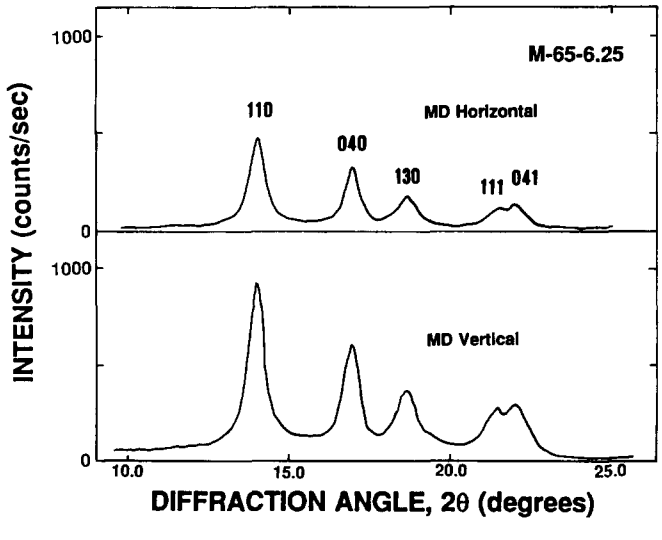

Figure 14 Wide-angle X-ray diffraction patterns of the web M-65-6.25 with its MD in horizontal and vertical directions

associated with the annealing effect due to a slow crystallization[22]. More annealing of the crystals is possible at a short *DCD* and at a high die temperature. It should be noted that only a small amount of room-temperature air is involved in the melt blowing at a short *DCD* and thus the fibres are quenched slowly (*Figure 1*). As the DCD was increased, the annealing effect disappeared as shown by the bottom three d.s.c. curves in *Figure 13*, because more room-temperature air is involved at an increased *DCD* and the fibres quench rapidly. The melting endotherm becomes broad, and shifted to a lower temperature, as the *DCD* is increased. The area of the melting endotherms slightly decreased with increasing *DCD*, or with decreasing die temperature. The percentage of crystal calculated from the area of the melting endotherm was in the range of 39–44% using the heat of fusion of 45.0 cal g^{-1} (refs. 23–25) for the polypropylene monoclinic α-form crystal.

In *Figure 14*, wide-angle X-ray diffraction patterns of a melt-blown PP web with its MD along horizontal and vertical directions are shown. The first five diffraction peaks were identified as 1 1 0, 0 4 0, 1 3 0, 1 1 1 and 0 4 1 of the α-form crystal[26,27]. The intensity of the first five peaks are slightly greater when MD was in the vertical direction than when MD was in the horizontal direction. The web sample in *Figure 14* was produced at *DCD* of 0.16 m and showed a considerable fibre orientation along MD in the SEM photographs. Therefore, *Figure 14* suggests that polypropylene molecules are only slightly oriented in the fibres of the melt-blown web. Indeed, birefringence of individual fibres in various melt-blown PP webs have been previously measured, and found to be smaller than melt-spun fibres[13,15,18], indicating a low molecular orientation. Previous WAXD using flat X-ray films on PP melt-blown webs also showed no significant preferred crystal orientation[18,28].

In *Figure 15*, WAXD patterns of melt-blown webs produced at various *DCD* are shown. The diffraction pattern of the web at *DCD* of 0.16 m shows the α-form crystal like the sample M-65-6.25 in *Figure 14*. However, the diffraction pattern becomes broader and shows a considerable contribution from the smectic phase as *DCD* was increased. The smectic phase is disordered and metastable. The isotactic PP chains in the smectic phase are in a 3/1 helix conformation, but are arranged in a disordered fashion[29,30]. Usually the smectic phase of PP is obtained by fast quenching from the melt. The percentage of smectic phase in a sample has been found

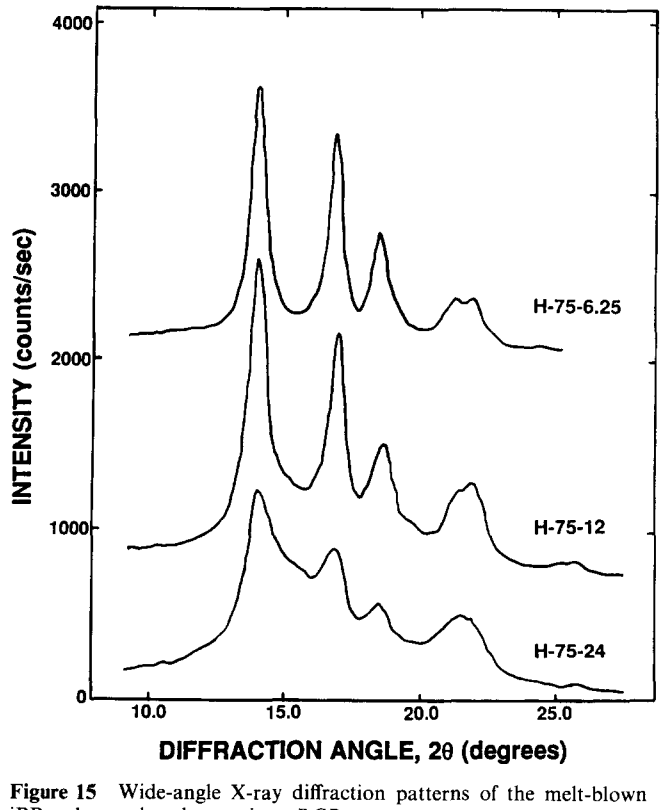

Figure 15 Wide-angle X-ray diffraction patterns of the melt-blown iPP webs produced at various *DCD*

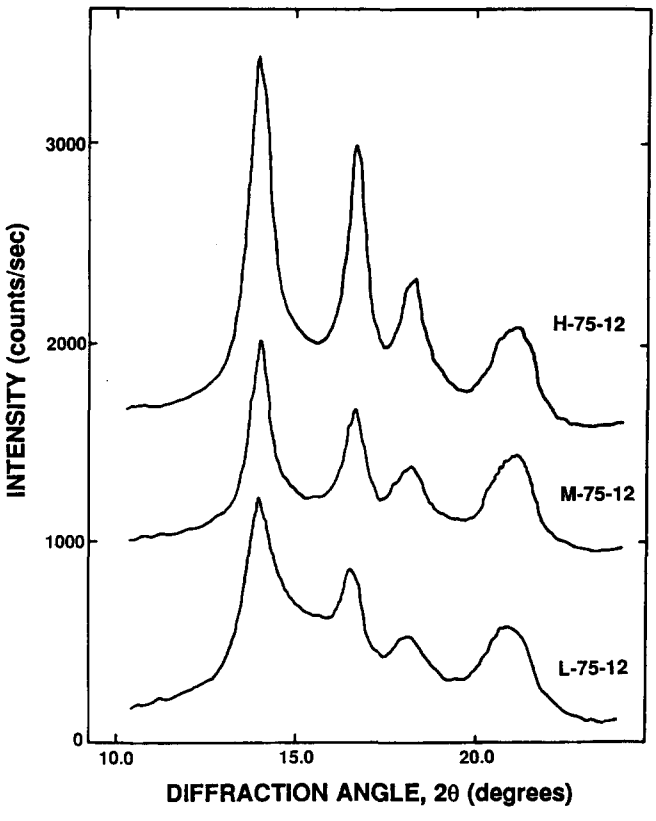

Figure 16 Wide-angle X-ray diffraction patterns of the melt-blown iPP webs produced at various die temperatures

to depend on the quenching conditions[31]. As *DCD* was increased, more room-temperature air was involved in the melt-blowing process, with the hot air stream from the die. Therefore, the quenching rate is faster. WAXD of H-75-6.25, H-75-12 and H-75-24 in *Figure 15* are similar to WAXD of the PP samples CR100, CR35 and CR0 in ref. 31, respectively. The samples CR100, CR35 and CR0 were prepared by quenching from the melt into a water bath at 100, 35 and 0°C, respectively. Some difference in sample preparation should be noted. In ref. 31, a 200 μm thick film with a thick copper substrate was quenched in a water bath. However, in this study, microdenier fibres with diameters ranging from 0.5 to 20 μm are cooled at a high speed. The percentages of α-form/smectic phase/amorphous regions of the samples of CR100, CR35 and CR0 were reported to be 61/0.0/39, 32/26/42 and 10/48/42, respectively. Although the existence of smectic phase in air-quenched PP webs was not considered, WAXD of melt-blown PP webs produced at 0.91 m clearly showed more smectic phase than the webs at 0.20 m[18]. The smectic phase has been observed in melt-spun PP fibres at a fast quenching condition, or at a low spinline stress[32–34].

Figure 16 shows WAXD of webs produced at various die temperatures. As the die temperatures decreased, the fraction of smectic phase increased owing to increased quenching rate. The fraction of smectic phase appeared to increase slightly with decreasing air flow rate owing to increased quenching rate. However, the effect of air flow rate on the fraction of smectic phase appeared to be smaller than that of die temperature or *DCD*. The above discussion of WAXD patterns in terms of the smectic phase were found for all the samples studied. Smectic phase was found to transform rapidly to α-form above 70°C[29,35]. This is the reason why similar areas of melting endotherms were observed for all the samples regardless of the fraction of smectic phase. The crystallinity of melt-blown PP webs has been reported by using d.s.c.[17,18]. As discussed above, the crystallinity from d.s.c. can be erroneously overestimated owing to the smectic–crystal transformation if the original sample has the smectic phase.

CONCLUSIONS

Isotactic polypropylene (iPP) webs melt blown at various processing conditions were investigated in terms of the macroscopic and microscopic structures and mechanical properties. The degree of fibre entanglement observed from scanning electron microscopy was increased with decreased die-to-collector distance (*DCD*), with increased die temperature, or with increasing air temperature. A broad range of fibre diameters was observed in all the webs studied. The average fibre diameter decreased with increasing processing temperature, or with increasing air flow rate, but did not appear to change much with *DCD*. A wide range of tensile properties and flexural rigidity can be obtained for PP webs by changing one of the three major processing conditions, i.e. die temperature, air flow rate and *DCD*. In general, increasing temperature and increasing air flow rate showed the same effects on tensile properties and flexural rigidity; they increased tenacity and flexural rigidity. These findings can be used to reduce the energy requirement of the melt-blowing process. Using wide-angle X-ray diffraction, melt-blown PP webs were found to consist of α-form crystals, smectic phases and amorphous regions. The fraction of the smectic phase increased with increasing *DCD* or decreasing die temperature. Since the smectic phase transforms to crystals on heating ($\sim$70°C), the crystallinity of PP webs obtained from differential scanning calorimetry showed 39–44% regardless of the fraction of smectic phase.

ACKNOWLEDGEMENTS

The authors express appreciation to Exxon Chemical Company for funding and permission to publish the results of this research. We appreciate the encouragement and support of Dr W. J. McCulloch, Exxon Chemical Company. We acknowledge the contribution of Mr R. A. Meade, Mr L. E. Spires and Ms N. Castillo to this research.

REFERENCES

1 Van Wente, A. *Ind. Eng. Chem.* 1956, **48**, 1342
2 Lee, Y. and Wadsworth, L. C. *Polym. Eng. Sci.* 1990, **30**, 1413
3 Wadsworth, L. C., Lee, Y. and Barbuza, S. D. *J. Nonwoven Res.* 1990, **2** (1), 43; *Proc. INDA Tech. Symp.* 1989, **17**, 585
4 Dever, M., Wadsworth, L. C. and Lee, Y. *Proc. INDA Tech. Symp.* 1990, **18**, 1
5 McCulloch, W. J. and Van Brederode, R. A. Insight 81, Absorbent Products Conference, San Antonio, Texas, 1981
6 Buntin, R. R. *Tappi* 1973, **56** (4), 74
7 Buntin, R. R. US Patent 3972759 (1976)
8 Buntin, R. R., Keller, J. P. and Harding, J. W. US Patent 3849241 (1974)
9 Schwarz, E. C. A. US Patent 4380570 (1983)
10 Bringman, D. J. and Buntin, R. R. Society of Plastics Industry, 32nd Annual Technical Conference, San Francisco, CA, 1974

11 Wadsworth, L. C. and Jones, A. M. *Nonwovens Industry* 1986, **17**, 44
12 Jones, A. M. and Wadsworth, L. C. Tappi Nonwovens Conference, Atlanta, April 1986
13 Choi, K. J., Spruiell, J. E., Fellers, J. F. and Wadsworth, L. C. *Polym. Eng. Sci.* 1988, **28** (2), 81
14 Milligan, M. W., Wadsworth, L. C. and Cheng, C. Y. *Proc. INDA Tech. Symp.* 1989, **17**, 573
15 Straeffer, G. and Goswami, B. C. *Proc. INDA Tech. Symp.* 1990, **18**, 385
16 Thompson, D. R., Clark, J. C. and Crater, D. H. *Proc. INDA Tech. Symp.* 1990, **18**, 345
17 Narasimhan, K. M. and Shambaugh, R. L. *Proc. INDA Tech. Symp.* 1987, **15**, 189
18 Bodaghi, H. *Proc. INDA Tech. Symp.* 1989, **17**, 535
19 Bergmann, L. *Nonwovens Industry* 1988, **19**, 26
20 'Annual Book of ASTM Standards', American Society for Testing and Materials, Philadelphia
21 'INDA Standard Tests', Association of the Nonwoven Fabrics Industry, Cary, NC
22 Wunderlich, B. 'Macromolecular Physics', Academic Press, New York, 1980, Vol. 3
23 Brandrup, J. and Immergut, E. H. 'Polymer Handbook', 2nd Edn, Wiley, New York, 1975
24 Danusso, F. and Gianotti, G. *Eur. Polym. J.* 1968, **4**, 165
25 Passaglia, E. and Kevorkian, H. K. *J. Appl. Phys.* 1963, **34**, 90
26 Turner-Jones, A., Aizlewood, J. M. and Beckett, D. R. *Makromol. Chem.* 1964, **75**, 134
27 Natta, G. and Corradini, P. *Nuovo. Cimento Suppl.* 1960, **15**, 40
28 Lee, Y. and Wadsworth, L. C. to be published
29 Saraf, R. and Porter, R. S. *Mol. Cryst. Liq. Cryst. Lett.* 1985, **2**, 85
30 Miller, R. L. *Polymer* 1960, **1**, 135
31 Vittoria, V. and Perullo, A. *J. Macromol. Sci. (B)* 1986, **25**, 267
32 Lu, F. M. and Spruiell, J. E. *J. Appl. Polym. Sci.* 1987, **34**, 1521
33 Sheehan, W. C. and Cole, T. B. *J. Appl. Polym. Sci.* 1964, **8**, 2359
34 Nadella, H. P., Henson, M. M., Spruiell, J. E. and White, J. L. *J. Appl. Polym. Sci.* 1977, **21**, 3003
35 Zanetti, R., Celotti, G., Fichera, A. and Francesconi, R. *Makromol. Chem.* 1969, **128**, 137